Overcoming Insulin Insufficiency by Forced Follistatin Expression in β-cells of *db/db* Mice

Chunxia Zhao[1,2], Chunping Qiao[1], Ru-Hang Tang[1], Jiangang Jiang[2], Jianbin Li[1], Carrie Bette Martin[1], Karen Bulaklak[1], Juan Li[1], Dao Wen Wang[2] and Xiao Xiao[1]

[1]Division of Molecular Pharmaceutics, Eshelman School of Pharmacy, University of North Carolina, Chapel Hill, North Carolina, USA; [2]Cardiovascular Division of Internal Medicine, Tongji Hospital, Tongji Medical College, Huazhong University of Science and Technology, Wuhan, China

Diabetes poses a substantial burden to society as it can lead to serious complications and premature death. The number of cases continues to increase worldwide. Two major causes of diabetes are insulin resistance and insulin insufficiency. Currently, there are few antidiabetic drugs available that can preserve or protect β-cell function to overcome insulin insufficiency in diabetes. We describe a therapeutic strategy to preserve β-cell function by overexpression of follistatin (FST) using an AAV vector (AAV8-Ins-FST) in diabetic mouse model. Overexpression of FST in the pancreas of *db/db* mouse increased β-cell islet mass, decreased fasting glucose level, alleviated diabetic symptoms, and essentially doubled lifespan of the treated mice. The observed islet enlargement was attributed to β-cell proliferation as a result of bioneutralization of myostatin and activin by FST. Overall, our study indicates overexpression of FST in the diabetic pancreas preserves β-cell function by promoting β-cell proliferation, opening up a new therapeutic avenue for the treatment of diabetes.

Received 21 November 2014; accepted 4 February 2015; advance online publication 10 March 2015. doi:10.1038/mt.2015.29

INTRODUCTION

Diabetes is a chronic metabolic disorder characterized by hyperglycemia as a result of insulin deficiency and/or damaged tissue response to insulin.[1,2] Traditional antidiabetic treatments mainly focus on glycemic control via administration of insulin or improving the tissue response to insulin.[3,4] In fact, it is the β-cell deterioration that determines the rate and prognosis of the disease.[5,6] Because there are few drugs available that can preserve or protect β-cells, any such therapy would revolutionize diabetes treatment. One of the most recent advancement in antidiabetic medication is the use of incretin-based therapies (*i.e.*, glucagon-like peptide-1 receptor agonists and dipeptidyl peptidase-4 inhibitors[7,8]). Glucagon-like peptide-1 receptor agonists increase insulin secretion in a glucose-dependent manner, resulting in a low risk of hypoglycemia, and more importantly, offering a weight loss benefit when compared with insulin administration.[9] Nevertheless, the glucagon-like peptide-1 receptor agonists have limited effects in human β-cells.[7,10]

Follistatin (FST) emerges as a potential therapeutic candidate for preserving or protecting islet β-cell function. Originally recognized as an inhibitor of follicle-stimulating hormone, FST plays important roles in embryonic development, as well as in the proper functioning of the reproductive, endocrine, and musculoskeletal systems.[11–13] FST has earlier been used as an effective treatment for muscle degenerative diseases by increasing muscle fiber sizes through binding and bioneutralization of transforming growth factor (TGF)-β superfamily members.[14,15] Although the role of FST in the musculoskeletal system is clearly defined, information regarding the specific involvement of FST in pancreatic development and β-cell function is scarce and contains some degree of contradiction.[14,16,17]

Although the general consensus is that FST and its binding partners play important roles in the adult pancreas, some ambiguity remains because of its complicated binding ligands, different and overlapping ligand receptors, and a multitude of downstream effectors.[18] For example, activin A is antagonized by FST, yet is important in pancreatic development and controlling insulin secretion.[19,20] On the other hand, overexpression of FST may prove to be an effective treatment strategy for obesity and diabetes, as mice deficient in SMAD3 (Sma- and Mad-related protein 3, a critical mediator of the TGF-β signaling pathway) exhibited increased circulating insulin levels and consequently decreased levels of blood glucose.[21] Nevertheless, no direct evidence of the function of FST on β-cell in the pancreas currently exists.

In this study, we sought to investigate whether overexpression of FST in the pancreas preserves β-cell function in type 2 diabetic mouse models. The mouse FST gene was driven by insulin promoter to achieve β-cell specific transgene expression, and the adeno-associated virus serotype 8 (AAV8) vector was used to obtain robust transgene expression in the pancreas.[22] Our results showed that long-term overexpression of FST in the pancreas of *db/db* mice promoted β-cell proliferation and maintained pancreatic islet mass. *db/db* mouse is a leptin receptor deficient type 2 diabetes model. The function of leptin hormone is to regulate hunger and energy expenditure by acting on its receptor in the hypothalamus and peripheral targets. The absence of leptin receptor in the *db/db* mice leads to metabolic syndrome with severe obesity and type 2 diabetes.[23] The treatment also ameliorated hyperglycemia, relieved diabetic symptoms, and prolonged life span of the diabetic *db/db* mice despite the presence of obesity. We found that FST treatment inhibited SMAD2/3 signaling and consequently activated insulin-phosphoinositide 3-kinase (PI3K)-Akt pathway.

The first two authors contributed equally to this work.

Correspondence: *Xiao Xiao, Division of Molecular Pharmaceutics, Eshelman School of Pharmacy, University of North Carolina, Chapel Hill, North Carolina 27599, United States. E-mail: xxiao@email.unc.edu*

These results are consistent with our hypothesis that FST plays an important role in maintaining glucose homeostasis by promoting β-cell proliferation in diabetic mice. Thus, overexpression of FST represents a novel therapeutic strategy for type 2 diabetes.

RESULTS

AAV8-Ins-FST delivery ameliorates diabetic symptoms and extends lifespan of *db/db* mice

To evaluate the function of FST in the islets of diabetic mice, the AAV8-Ins-FST vector (5×10^{11} vg/mouse) was delivered into 6-week-old *db/db* mice ($n = 5$) via intraperitoneal injection. Our earlier study indicated that intraperitoneal. injection of AAV8 vector driven by an insulin promoter rendered strong and highly specific gene expression in ββ-cells.[24] FST expression in the pancreas was determined by both real-time PCR and immunofluorescent (IF) staining. FST expression in the pancreas is naturally low in the wild-type C57BL/6 mouse.[25] FST mRNA is even lower in the pancreas of *db/db* mice (0.16 ± 0.08) when compared with that of the wild-type mice. AAV8-Ins-FST treatment resulted in a significant increase of FST mRNA (**Figure 1a**). The relatively low follistatin expression revealed by IF staining (**Figure 2a**, green) was mainly due to the secretable nature of the protein and relative long period of time post vector delivery (the mice were sacrificed at 8.5 months of age). Because diabetes is characterized by hyperglycemia, polyuria, polydipsia, and sometimes polyphagia, we monitored blood glucose, water, and food intake in both treated and untreated mice. Blood glucose in treated mice began to drop significantly as early as 2 weeks after treatment (292 ± 70.46 mg/dl in treated group versus 403 ± 41.03 mg/dl in control group, $n = 5$, $p = 0.008$), and reached to 155 ± 35 mg/dl in treated group at ~1 year after treatment (**Figure 1d**). Meanwhile, water intake (**Figure 1e**) and food intake (**Figure 1f**) were also significantly reduced in treated mice (109.73 ± 1.5 g/kg/day for food, 12.2 ± 1.5 ml/day for water, $n = 5$) when compared with their untreated counterparts (151.81 ± 3.9 g/kg/day for food, $n = 4$, $P = 0.00003$, 19.73 ± 1.22 ml/day for water, $n = 3$, $p = 0.009$) at 20 weeks after treatment.

We also investigated the effects of overexpression of FST on severe diabetes by delivering the vector into 5-month-old *db/db* mice, which showed very severe hyperglycemia and also started to have diminished insulin production. This therapeutic regimen resembles current clinical practice whereby treatment is given after the disease manifestation. The AAV8-Ins-FST vector (5×10^{11} vg/mouse) was administered intraperitoneally. to the 5-month-old *db/db* mice ($n = 4$) and the age-matched untreated *db/db* mice were used as controls. The onset of the therapeutic effect of FST appeared delayed in the aged group compared to the younger-treated group mentioned earlier. At 11 months post-treatment, blood glucose levels of the treated group steadily dropped to 145.5 ± 56 mg/dl; however, none of the control *db/db* mice survived past 5 months after treatment (**Figure 1g**). Similar to the phenomenon observed in the younger-treated group, water and food intake were also significantly decreased by the treatment (**Figure 1h**, **i**). Overall, these results suggest that overexpression of FST in pancreatic β-cells can alleviate glucose homeostasis impairment and ameliorate diabetic symptoms in *db/db* mice.

Finally, the important characteristic of *db/db* mice is their short life span. The average life span of the untreated *db/db* mice was 242.4 ± 80.79 days ($n = 19$), whereas the average life span of the treated *db/db* mice was almost doubled to 427.56 ± 44.95 days ($n = 9$, $p < 0.0001$) (**Figure 1b**), although their body weights were even greater than the untreated *db/db* mice (**Figure 1c**). The metabolism was slower in the treated *db/db* mice when compared with the that of the untreated counterpart (**Supplementary Figure S2**). This data clearly indicates that overexpression of FST improves survival of *db/db* mice despite the presence of obesity.

Because insulin deficiency is a key culprit in diabetes progression, we examined the impact of our treatment on serum levels of insulin. Similar to type 2 diabetes patients, the untreated *db/db* mice were hyperinsulinemic during the early stages of the disease. Insulin serum levels of the *db/db* control mice at 3 months of age was higher than normal C57BL/6 mice (5.98 ± 2.91 μg/l versus 1.04 ± 0.43 μg/l, respectively, $P = 0.002$), and serum insulin levels of the *db/db* mice declined with age (**Figure 3a**). When the *db/db* mice reached the end stage of the disease, insulin levels decreased to 1.69 ± 0.61 μg/l at 8–9 months of age. On the other hand, the serum insulin level of treated *db/db* stayed high and did not decrease over time. Serum insulin level of the treated mice was (8.52 ± 4.69 μg/l) at 3 months of age and remained high at 10.26 ± 0.71 μg/l at 14 months of age (**Figure 3a**). Insulin expression (β-cell cytoplasmic insulin) in the pancreas was confirmed by real-time PCR, IF staining and Western blot. The mRNA expression of insulin in the pancreas of treated *db/db* mice was increased by 27.7-fold when compared with that of control mice (**Figure 3b**). IF staining revealed more insulin-positive cells in the treated group (**Figure 2a**,**b**), whereas Western blot showed much stronger insulin expression than the controls (**Figure 3c**). It should be noted that insulin synthesized and stored in the β-cells of treated *db/db* mice was still lower than that of the wild-type C57/BL6 mice (**Figure 3c**), although their serum insulin levels were higher.

FST treatment increased islet size by promoting β-cells proliferation

Prevention of β-cell decline is a key issue in type 2 diabetes mellitus treatment.[6,26] To elucidate the effect of our treatment in this context, we sacrificed experimental mice at 8.5 months ($n = 3$) and 15 months of age ($n = 2$). We observed a substantial increase in islet size with treatment as compared to control *db/db* mice and normal *C57BL/6* mice (3.3-fold over *db/db*, $P = 0.001$, $n = 4$; 1.8-fold over *C57BL/6*, $P = 0.01$, $n = 4$) (**Figure 4a**). Correspondingly, the ratio of islet to pancreas area was also significantly increased in treated mice (4-fold over *db/db* mice, $P = 0.001$; 1.8-fold over C57BL/6 mice, $P = 0.02$, $n = 4$) (**Figure 4b**). We next examined whether the treatment could improve the composition of islet cell type. To analyze cellular composition, double IF staining was performed against antibodies of insulin (β-cell) and glucagon (α-cell) or somatostatin (δ-cell) on paraffin embedded tissues (**Figure 2b**). Quantification data for the control *db/db* mice shows a decreased β-cell mass (40.9 ± 5.54%, $n = 4$, $P = 0.004$) (**Figure 4c**) and increased α-cell (33.4 ± 4.59%, $n = 4$, $p = 0.0004$) (**Figure 4d**) and δ-cell (25.7 ± 4.14%, $n = 4$, $P = 0.002$) (**Figure 4e**) mass when compared with normal C57BL/6 mice (61.7 ± 0.42%, 19.13 ± 2.19%, 13.18 ± 1.91% of β-, α-, and δ-cell ratios, respectively). Remarkably, the AAV8-Ins-FST treatment completely normalized the β-cell (63.28 ± 5 .65%) and δ-cell (11.53 ± 2.16%) percentage (**Figure 4c**,**e**). The α-cell mass (23.6 ± 2.12%, $n = 4$,

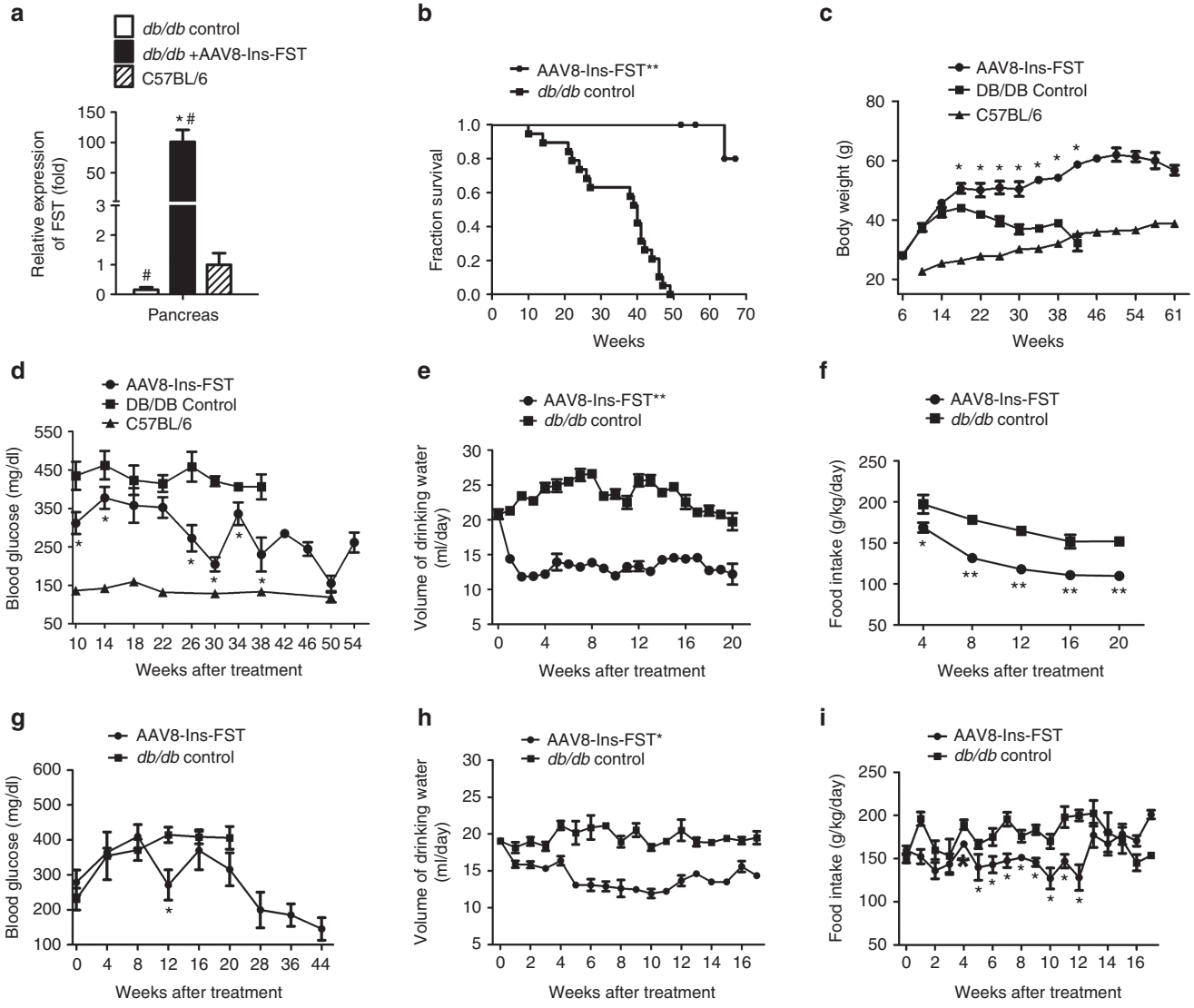

Figure 1 Delivering AAV8-Ins-FST into pancreatic β-cells alleviated diabetic symptoms and prolonged lifespan in both young and old *db/db* mice. (**a**) mRNA expression of FST in the pancreas of *db/db* control, treated mice, and wild-type at 8.5 months old. (**b**) The AAV8-Ins-FST treatment significantly improved longevity of the diabetic mice. (**c**) Body weight of the AAV8-Ins-FST treated mice was increased compared to the control group. (**d**) Blood–glucose levels were decreased after long-term treatment in young treated mice. Mice were fasted for 16 hours (fasting longer period to obtain reading from glucose meter of the control mice) prior to sample collection. (**e**) The young treated mice consistently drank less water than the untreated controls; $n = 3$ per group. (**f**) Food intake (measured by g/kg/day) was reduced in young treated mice; $n = 4$ per group. (**g**) Blood glucose level slowly but steadily decreased in the aged treatment group (treated at 5-month-old of age). The control group did not survive past 5 months post-treatment. (**h**) Aged *db/db* mice drank significantly less water after AAV8-Ins-FST treatment than the controls. (**i**) Food intake at older age was significantly less in the treated group than the control; $n = 5$ for all groups if not otherwise specified. $^{*}P < 0.05$ and $^{**}P < 0.005$ compared to *db/db* control mice; $^{\#}P < 0.05$ compared to the *C57BL/6* mice. Data are represented as mean ± SEM.

$P = 0.07$) was slightly increased in the pancreas of the treated *db/db* mice compared with that of the *C57BL/6* mice, but it was significantly improved when compared with the untreated *db/db* mice (**Figure 4d**). Therefore, AAV8-Ins-FST treatment increased islet size, number of β-cells, and normalized the β-cell to total islet cell ratio.

Potential mechanisms pertaining to preserved β-cell function include increasing β-cell proliferation or preventing cell death. To determine the contribution of cell proliferation, we performed coIF staining for proliferation marker Ki67 and β-cell marker insulin. Ki67 is a nuclear protein that is strictly associated with cellular proliferation.[27] As shown in **Figure 2c**, there were more Ki67 positive cells in islets of treated mice than that of the control *db/db* mice. The β-cell proliferation rate in treated mice averaged about 10-fold higher than in the control *db/db* mice (5.67 ± 1.72% versus 0.53 ± 0.45%, $n = 3$, $P = 0.02$) (**Figure 4f**). Costaining against Ki67 and glucagon (α-cell marker) in pancreas samples revealed that Ki67 positive cells were not glucagon-positive in both groups (**Figure 2d**), indicating that the proliferating cells were β-cells rather than α-cells in the treated islets. Notably, a few cells were positive for both insulin (red) and glucagon (green) (**Figure 2e**) in treated mice. These bihormonal cells (yellow) may either be undefined precursors that started to produce two hormones or pre-existing α-cells that started producing insulin, or both.[28]

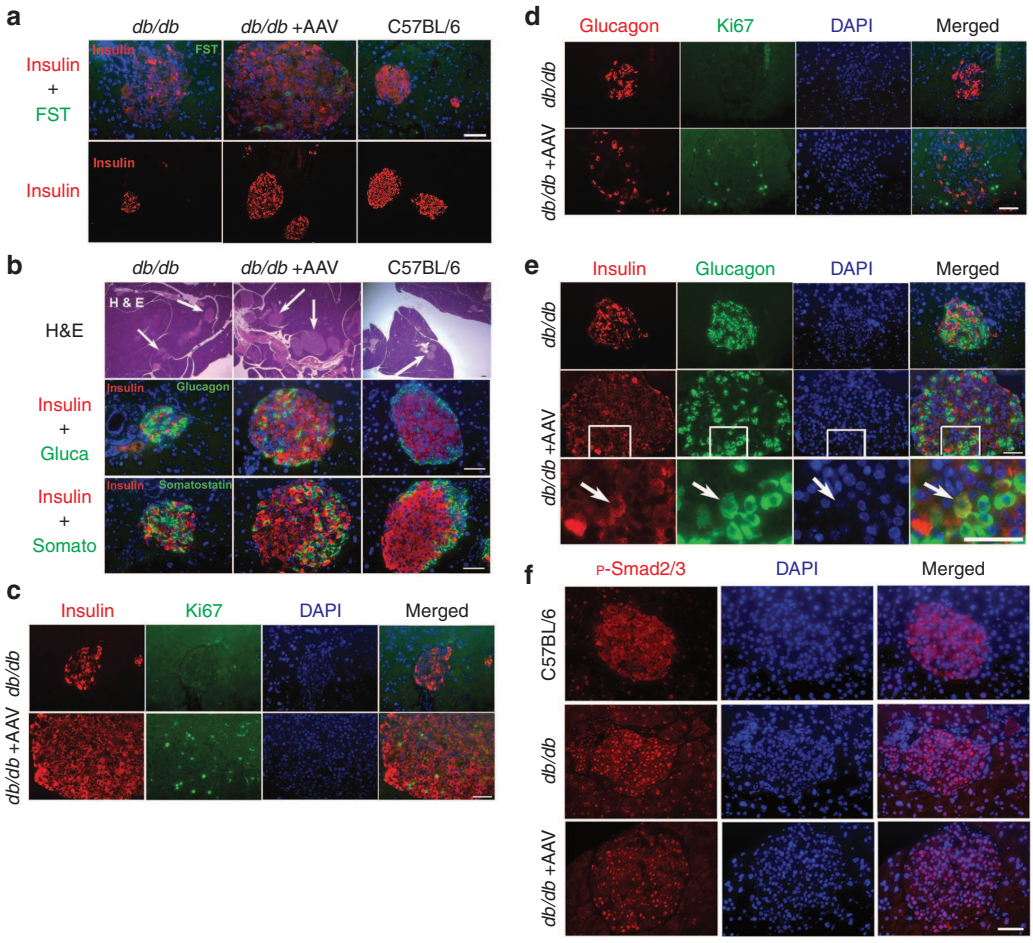

Figure 2 Immunofluorescent staining of different markers in control and treated pancreas. Displayed are single or multiple pancreatic islets. Nuclei were stained with 4′,6-diamidino-2-phenylindole (DAPI) (blue). Individual scale bar (50 µm) are labeled to show the magnification scale. (**a**) Costaining of insulin (red) and FST (green) in the pancreas. (**b**) Morphology examination and IF staining against insulin (red), glucagon (green), and somatostatin (green) in the pancreatic islets. (**c**) Costaining of cell proliferation marker Ki67 (green) and β-cell marker insulin (red). (**d**) Costaining of cell proliferation marker Ki67 (green) and α-cell marker glucagon (red). (**e**) Costaining of insulin (red) and glucagon (green) shows some bihormonal (producing both insulin and glucagon, as shown by arrow) cells in AAV8-Ins-FST-treated mice. Nuclei were stained with DAPI (blue). Bottom row is magnified from middle pictures (as indicated by box and white arrow head) to show further detail. (**f**) Immunofluorescence staining of phospho-SMAD2/3 in the pancreas. For most of the figures applied, nuclei were stained with DAPI (blue). Scale bar: 50 µm.

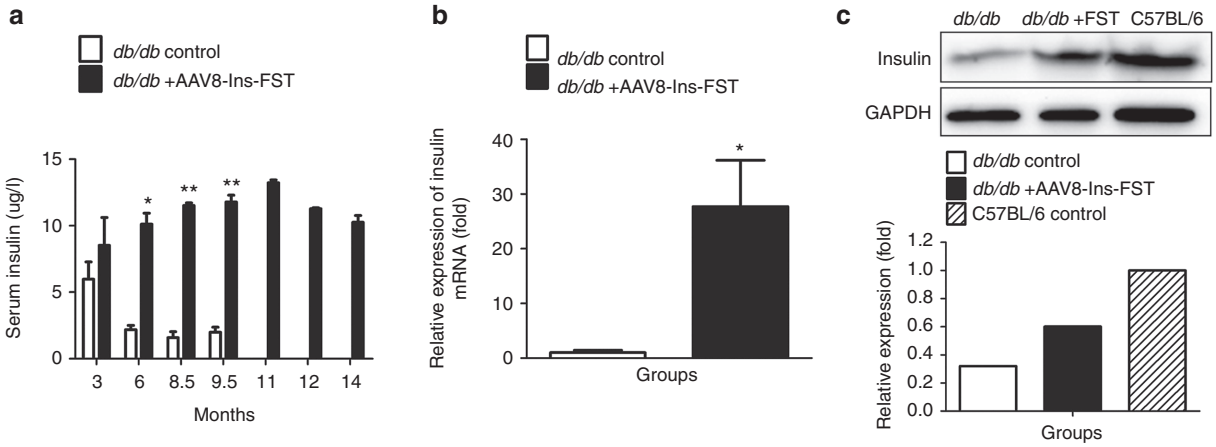

Figure 3 Delivering AAV8-Ins-FST into pancreatic β-cells improved serum insulin levels. (**a**) AAV8-Ins-FST treatment at 5–6-week-old mice improved serum insulin levels in *db/db* mice ($n = 5$ for each group). (**b**) Levels of insulin mRNA were measured by RT-PCR and found to have increased 27.7-fold in the treated pancreas as compared to the untreated pancreas ($P = 0.0067$, $n = 5$). Samples were taken from mice sacrificed at 8.5 months old. (**c**) Western blot analysis showed increased insulin expression in the treated islets compared to islets from untreated *db/db* mice. Insulin expression in wild-type C57BL/6 mice was greater than in the treated *db/db* mice ($n = 3$ for each group). The samples were from pooled islets of three mice. *$P < 0.05$ or **$P < 0.005$ compared to untreated mice. Data is represented as mean ± SEM.

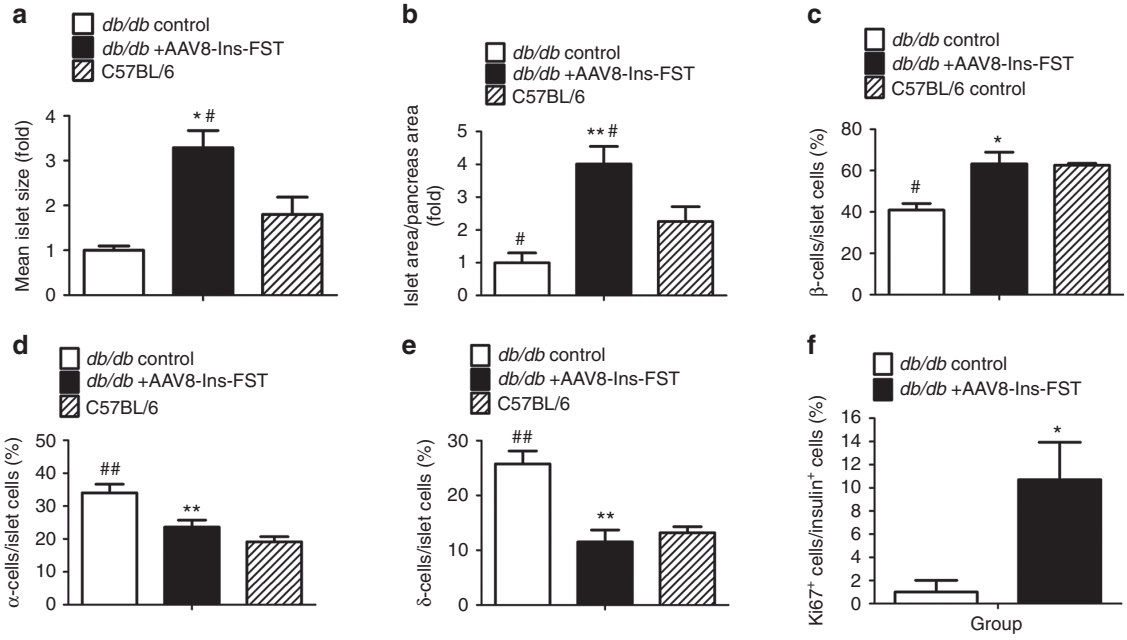

Figure 4 Overexpression of follistatin (FST) in pancreatic β-cells increased islet numbers and mass, and normalized composition of islet cell types in *db/db* mice. (**a**) Mean islet size in the pancreas. Islet area was calculated using H&E images (10×) and positively-labeled pixels were quantified with Adobe Photoshop 7.0 software ($n = 4$ for each group). All islets were imaged. (**b**) The ratio of islet to total pancreas area was significantly increased in the AAV8-Ins-FST treated pancreas ($n = 4$ for each group). (**c**) Delivering AAV8-Ins-FST into the pancreas of *db/db* mice normalized the β-cell to total islet cell ratio. For each mouse, about 10,000 β-cells were counted, and there were four mice in each group. (**d**) α-cell to total islet cell ratio was decreased in the treated *db/db* mice as compared to the untreated *db/db* mice. (**e**) Treatment of AAV8-Ins-FST normalized δ-cell to total islet cell ratio in the pancreas of *db/db* mice. (**f**) Percentage of $Ki67^+$ cells to $insulin^+$ cells in the islets ($n = 5$ for AAV8-Ins-FST treated group, and $n = 4$ for *db/db* control group). $^*P < 0.05$ and $^{**}P < 0.005$ compared to *db/db* control mice; $^{\#}P < 0.05$ and $^{\#\#}P < 0.005$ compared to the C57BL/6 mice. Data are represented as mean ± SEM.

Inhibition of SMAD pathway and activation of the PI3K-Akt pathway

To understand the molecular mechanisms underlying the β-cell proliferation observed following FST treatment, Western blot and IF staining were performed to detect relevant signaling pathways. In particular, the TGF-β-SMAD (Sma and Mad-related proteins) and the insulin-PI3K-Akt pathways were investigated. TGF-β superfamily ligands function through binding to cell surface complexes, and different types of ligands trigger phosphorylation of distinct receptor-mediated SMADs.[29,30] The TGF-β ligands activin, myostatin, and nodal induce phosphorylation of SMAD2/3, whereas bone morphogenetic proteins (BMPs) ligand binding will result in phosphorylation of SMAD1/5/8.[31] The level of phosphorylated SMAD2/3 (p-SMAD2/3) and SMAD1/5/8 (p-SMAD1/5/8) in the treated versus untreated pancreas were revealed by IF staining. Both p-SMAD2/3 and p-SMAD1/5/8 were significantly upregulated in the *db/db* pancreas as compared to the normal *C57BL/6* pancreas (**Figure 2f**, **Supplementary Figure S1**). AAV8-Ins-FST treatment significantly inhibited SMAD2/3 signaling (76.3 ± 1.5% of p-SMAD2/3 cells in the treated *db/db* islets versus 95.3 ± 0.78% in untreated *db/db* islets, $P = 0.0002$, $n = 3$) (**Figure 5a**) and had less nuclear localization of p-SMAD2/3(**Figure 2f**), whereas SMAD1/5/8 signaling was slightly altered (66.1 ± 3.9% of p-SMAD1/5/8 cells in the treated *db/db* islets versus 76.7 ± 4.9% in untreated *db/db* islets, $P > 0.05$, $n = 3$) (**Figure 5b** and **Supplementary Figure S1**). This indicates the therapeutic effects of FST on islets are mainly through inhibition of SMAD2/3 pathway via bioneutralizaiton of myostatin, activin, or nodal. It is unclear whether SMAD1/5/8 pathway was also inhibited in our study.

The PI3K-Akt pathway plays a critical role in the regulation of β-cell mass in the pancreas and defects in this signaling pathway have been shown to contribute to type 2 diabetes.[32] To reveal the effect of FST treatment on this pathway, the pancreatic islets were isolated, pooled, and subjected to Western blot. Phosphorylated PI3K (p-PI3K) in the FST-treated pancreatic islets was greater than the untreated *db/db* islets (**Figure 5c**). Similarly, the total AKT and phosphorylated AKT (p-Akt) were both higher in islets isolated from FST-treated *db/db* mice compared with the untreated controls (**Figure 5c**,**d**). Collectively, these results indicate that FST overexpression activates the insulin-PI3K-Akt signaling pathway.

Potential binding ligands of FST in the treated pancreas

To identify the targeting ligand(s) of FST in the treated pancreas, real-time PCR and real-time PCR array of the murine TGF-β/BMP signaling pathway were performed on pancreatic cDNA from treated and control mice. Myostatin mRNA was significantly upregulated in the AAV8-Ins-FST-treated pancreas (**Figure 6a**). It is well known that myostatin gene expression is auto-regulated by a negative feedback mechanism.[33] Therefore, the observed increase of myostatin mRNA in the treated pancreas indicates myostatin inhibition. In a similar fashion, activin (inhibin β_A) mRNA was significantly upregulated in the treated pancreas (**Figure 6a**). In addition, we also noticed the mRNAs of two activin antagonists, BAMBI (BMP and activin membrane-bound inhibitor)

and inhibin-α, were upregulated (**Figure 6a**). BAMBI encodes a pseudo type I receptor, but lacks an intracellular kinase domain required for signaling, thereby functioning as a general negative regulator of TGF-β/BMP/activin signaling.[34] Inhibin blocks the function of activin through competitive binding of both type I and type II receptors.[35,36] Currently, it is unclear what mechanism drive the upregulation of BAMBI and inhibin-α mRNA expression in the FST-treated pancreas. The similar phenomenon, correlation of upregulation in BAMBI mRNA with a diminution in activin bioactivity, was observed at the time of gonocyte differentiation in germ cells.[37] Nevertheless, the increase in mRNAs of myostatin, activin, and two activin inhibitors suggests blockade of myostatin and activin in the AAV8-Ins-FST treated pancreas.

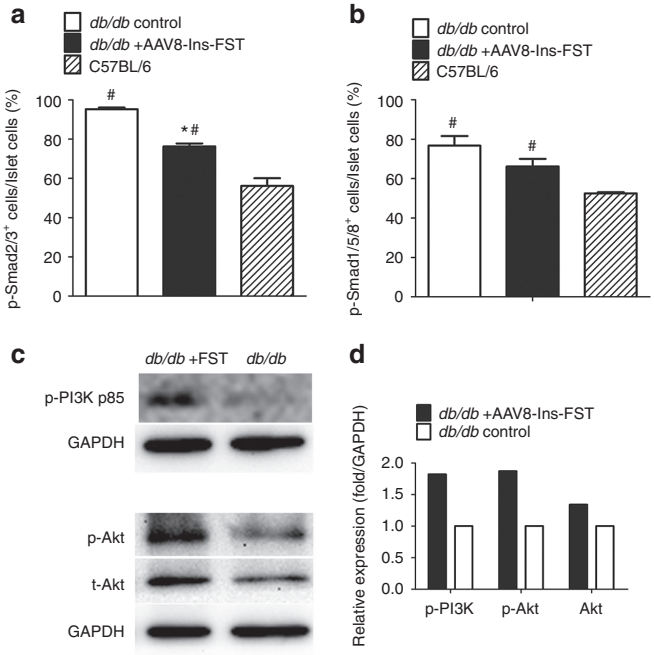

Figure 5 Inhibition of SMAD pathway and activation of the PI3K-Akt pathway. (**a**) Percentage of phospho-SMAD2/3 nuclear positive cells to total islet cells. (**b**) Percentage of phospho-SMAD1/5/8 nuclear positive cells to total islet cells. (**c**) The expression of phosphorylated PI3K (p-PI3K), phosphorylation of Akt (p-Akt, ser473), and total Akt (t-Akt) in FST-treated islets was higher than the untreated *db/db* islets as shown by Western blot ($n = 3$ for each group). The samples for Western blot were from pooled islets of three mice. (**d**) Semiquantitative analysis of Western blot results for p-PI3K, p-Akt, and t-Akt $^{*}P < 0.05$ compared to *db/db* control mice. $^{\#}P < 0.05$ compared to *C57BL/6* mice. Data are represented as mean ± SEM.

Proliferation of pancreatic β-cell was responsible for the steady and persistent serum insulin level in the AAV8-Ins-FST treated *db/db* mice of our study. We next asked what factors might promote β-cell proliferation in this context. Of particular interest, we noticed a significant increase of mitogenic factors betatrophin mRNA. Betatrophin is a newly identified hormone that promotes β-cell proliferation and improves glucose tolerance in mice.[27] Betatrophin mRNA was significantly upregulated in the AAV8-Ins-FST treated pancreas (47.1 ± 17.17 fold, $n = 3$, $P < 0.05$) (**Figure 6b**). We hypothesized that betatrophin could be transcriptionally repressed by activin, or myostatin, via SMAD3 pathway; therefore, overexpression of FST in the β-cell would increase betatrophin expression and promote β-cell proliferation.

To further test our hypothesis, an *in vitro* reporter plasmid Beta-Luc was constructed in which a secretable gaussia luciferase was driven by the betatrophin promoter (NCBI accession AC_000031, region 1910318–19105347). The Beta-Luc expression was evaluated in a mouse pancreatic β-cell line, NIT-1 cells. The Beta-Luc (Beta-Luc + pBSKS which is a control plasmid) elicited a significant amount of luciferase expression in the NIT-1 cells, peaking at 2 days (48 hours) post-transfection. Activin-conditioned media significantly inhibited luciferase expression to 26.8% ($n = 3$, $P = 0.0008$) at 48 hours (**Figure 6c**). Similarly, myostatin-conditioned media also inhibited luciferase expression (40.3%) at 48 hours, albeit to a less extent than the activin group (**Figure 6c**). As expected, FST plus activin or myostatin constructs partially recovered luciferase expression (50% for FST plus activin group versus 26.8% for activin alone, $n = 3$, $P = 0.05$ and 62.7% for FST plus myostatin group versus 40.3% for myostatin alone,

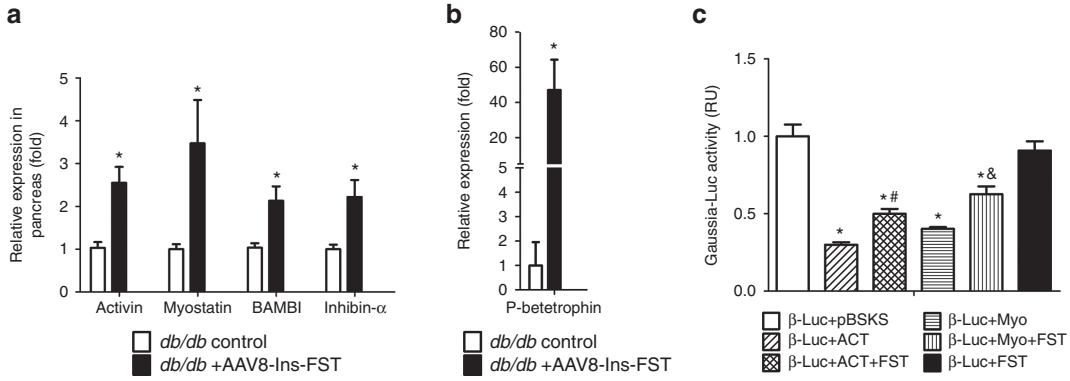

Figure 6 Promoting β-cell proliferation by inhibition of activin and myostatin via FST. (**a**) Relative mRNA expression of activin, myostatin, BAMBI, and inhibin-α by real-time PCR (or RT-PCR array) in the pancreas. (**b**) Relative mRNA expression of betatrophin in the pancreas by real-time PCR. (**c**) Inhibition of betatrophin expression by activin or myostatin shown using an *in vitro* reporter assay. NIT-1 cells were cotransfected with the mouse betatrophin promoter-luciferase plasmid (Beta-Gaussia-Luc), LacZ plasmid (transfection normalization control), and supplemented with conditional media for the indicated plasmids (refer to the section "Materials and Methods" for the details). pBSKS: bluescript control plasmid; ACT: activin plasmid driven by CB (Chick β-actin promoter with cytomegalovirus enhancer) promoter; FST: Follistatin plasmid driven by CAG promoter; Myo: myostatin plasmid driven by CB promoter. $^{*}P < 0.05$ compared to untreated control; $^{\#}P < 0.05$ compared to pEMBOL-ds-CB-Activin; $^{\&}P < 0.05$ compared to pEMBOL-ds-CB-myostatin. Data are represented as mean ± SEM.

$n = 3$, $P = 0.01$, **Figure 6c**). This *in vitro* reporter assay confirms our *in vivo* findings that overexpression of FST in the pancreas of diabetic mice increased mitogenic factor betatrophin expression by inhibition of activin and myostatin. This data also suggests that activin and myostatin can repress betatrophin transcription via acting on its promoter region in the pancreatic β-cells.

DISCUSSION

Diabetes is characterized by uncontrolled hyperglycemia and is linked to β-cell loss and dysfunction. Thus, preventing progressive loss of β-cell function is a key in treating diabetes. Here we describe a strategy to preserve and promote β-cell function via AAV-mediated overexpression of FST in the pancreas. Administration of AAV8-Ins-FST into pancreatic β-cells in *db/db* mice improved mouse lifespan, reduced serum glucose level, and ameliorated diabetic symptoms. The most important finding of our study was that overexpression of FST increased islet size by promoting β-cell proliferation in *db/db* mice. We demonstrated that this occurred through inhibition of the SMAD2/3 signaling and subsequent activation of insulin-PI3K-Akt pathway via bioneutralization by FST with its ligands, mainly myostatin and activin in the treated pancreas. Most likely FST315 specifically expressed in the β-cells functions mainly as a local autocrine regulator. However, minor paracrine effects could not be ruled out because FST is a secretable protein. Our *in vitro* reporter assay further indicated that activin and myostatin could negatively regulate the transcription of mitogenic factor betatrophin.[27] Although we observed an upregulation of betatrophin gene expression in the AAV FST-treated mice, the causative relationship between betatrophin expression and the observation of increased β-cell mass in our study remained unclear. Overexpression of FST in the pancreas of *db/db* mice might also increase some other mitogenic factors such as inhibitors of DNA binding proteins ID2 (data not shown).[38]

Controversial findings exist, highlighting the importance of further investigation. One report was from a follistatin like-3 (FSTL3) knockout study. FSTL3 and FST are structurally and functionally related glycoproteins that bind and antagonize actions of both activin and myostatin.[39] Homozygous FSTL3 knockout mice displays increased pancreatic islet numbers and sizes, β-cell hyperplasia, and enhanced glucose tolerance.[40] This phenomenon is quite different from what we have observed. Interestingly, FSTL3 knockout mice have opposite effects on glucose tolerance and insulin sensitivity compared to FST288-only mice, indicating FST and FSTL3 play different roles in regulating islet function and blood glucose homeostasis.[41] FST is translated as three protein isoforms: the full length circulating isoform FST315, the tissue-bound isoform FST288, and intermediate length gonad isoform FST303. They differ biochemically as well as in their distribution and mode of action. FST null mice are perinatally lethal; therefore, a mouse model that only expresses the tissue-bound FST288 isoform was made and viable to evaluate the role of tissue-bound FST in regulating adult body composition and glucose homeostasis.[41] In agreement with our findings, islet-specific SMAD3 knockout mice have increased insulin levels, decreased circulating glucose levels, and are protected from diet-induced obesity.[42] SMAD3 itself occupies the insulin gene promoter and represses insulin gene transcription.[42] In addition, islet-specific SMAD3 knockout mice have a more robust proliferative response after pancreatectomy.[43]

The conditional SMAD7 transgenic study is also worth mentioning.[44] SMAD7 is an inhibitory SMAD which blocks TGF-β signaling by blocking all the receptor-mediated SMAD phosphorylation and may also target TGF-β receptors for degradation.[45] SMAD7 expression in embryonic pancreas cells results in β-cell hypoplasia and neonatal lethality. These results actually do not contradict our findings, but emphasize the importance of balanced SMAD signaling in β-cell development and maturation. Furthermore, SMAD signaling may play a different role in regulating β-cell proliferation in normal and diseased pancreas.[46] SMAD inhibition may not be a strong stimulus for β-cell proliferation in a normal pancreas, where the signaling pathway is well balanced; however, it efficiently protects β-cell function in the diseased pancreas, where SMAD signaling is highly upregulated as revealed in our study.

The insulin-PI3K-Akt signaling pathway has been proven to play a critical role in the regulation of β-cell mass and function.[32,47,48] Some evidence of this can be seen in the insulin receptor substrate 2 (Irs2, a key upstream regulator of the PI3K/Akt signaling) knockout mice that show pathogenesis of type 2 diabetes as a consequence of combined insulin resistance and β-cell failure.[49] In addition, islets from type 2 diabetic patients exhibit reduced Irs2 expression, which supports the concept that altered Irs2-dependent signaling leads to β-cell failure in human patients.[50] In our study, FST treatment restored the PI3K-Akt pathway in the diabetic pancreas as seen by increased expression of p-P13K and Akt; therefore, the β-cell mass was increased, and diabetic symptoms were alleviated. However, the FST overexpression specifically in the pancreas, which we described in this study, was not sufficient to counteract peripheral insulin resistance. The treated *db/db* mice developed overt obesity in the end stage despite near-normal glucose level and increased insulin secretion, as seen in nondiabetic obesity.[51] On the other hand, systemic delivery of FST driven by ubiquitous promoter (which is out of scope of this manuscript) efficiently improved whole-body insulin sensitivity in addition to overcoming insulin insufficiency in the *db/db* mice. Future attempts of FST therapy may require ubiquitous expression of FST to overcome insulin insufficiency as well as insulin resistance.

Although we aimed to protect β-cell function via expressing therapeutic gene in pancreatic β-cells alone, we were surprised to find that FST treatment nearly doubled the lifespan of *db/db* mice. Our future direction will be to determine what factors attributed to this increased lifespan and how SMAD inhibition influences it. In summary, our study confirms that overexpression of FST in the pancreas can preserve β-cell function by promoting β-cell proliferation, presenting a novel therapeutic strategy for type 2 diabetes.

MATERIALS AND METHODS

Plasmid construction and AAV vector production. The mouse FST cDNA was generated by a RT-PCR method from a mouse ovary tissue. The sequences of the primers used are: 5′-CAG GAT GGT CTG CGC CAG -3′ and 5′-GTT TTG CCC AAA GGC TAT GTC-3′. By restriction digest with enzymes NotI and SalI, the cDNA fragment was cohesively ligated to the AAV backbone vector pEMBOL containing the insulin promoter. The final construct was named pEMBOL-D(+)-Ins-FST. AAV serotype 8 was chosen

as our delivery vehicle to achieve robust β-cell transgene expression,[22] and the final vector was named AAV8-Ins-FST. The AAV vector was produced by triple transfection method and the virus was purified by polyethylene glycol precipitation followed by CsCl centrifugation.[52] The titer of AAV vector was determined by both dot-blot and real-time PCR methods. The concentration of viral vector stock was in the range of 2×10^{12}–1×10^{13} vector genomes/ml.

Mice and vector administration. Male *db/db* (a rodent model of type 2 diabetes) and *C57BL/6* mice were purchased from the Jackson Laboratory at 4 weeks old. All animal protocols were approved by the University of North Carolina Animal Care and Use Committee. AAV8-Ins-FST vectors were delivered into the *db/db* mice at 6 weeks or 5 months old, by intraperitoneal injection at a final dose of 5×10^{11} vg/mouse.

Body weight, food, and water intake. Body weight was measured twice a month. Food intake and water intake were monitored for three times a week for 20 weeks after treatment.

Biochemical analysis. Blood glucose levels were measured using an ONETOUCH UltraSmart Blood Glucose Meter (LifeScan, New Brunswick, NJ, Cat # AW 060-795-01A). Blood was collected from the tail vein with a BD Microtainer Serum Seperator tube (REF 365956), and the serum was separated by spinning at 4 °C at 3000 RPM for 10 minutes in a micro centrifuge. Insulin concentrations were determined by ELISA using the Mercodia Mouse Insulin ELISA kit (Cat #10-1247-01).

Pancreas morphology and Immunohistochemistry. Pancreases were dissected at the indicated age, fixed with 4% paraformaldehyde and embedded in paraffin. H&E (hematoxylin and eosin) staining was performed on 5-μm paraffin sections using a previously reported method.[53] For IF staining, paraffin sections were dewaxed by heating for 1 hour at 60°C followed by soaking in xylene three times for 5 minutes each. Sections were rehydrated two times each for 5 minutes in 100%, 95%, 80% ethanol, once for 5 minutes in 70% and 50% ethanol, and finally 5 minutes in H_2O. They were then subjected to heat-mediated antigen retrieval (retrieval buffer: 10 mmol/l sodium citrate, 0.05% Tween 20, pH 6.0). The sections were permeabilized with permeabilization buffer (0.2% Triton X-100 in PBS) for 45 minutes at room temperature. After blocking (10% horse serum in PBS), the sections were incubated with various primary antibodies overnight. The following primary antibodies were used: rabbit anti-FST antibody (Santa Cruz, Dallas, TX, Cat# sc-30194), guinea pig anti-insulin antibody (Abcam, Cambridge, UK, Cat# ab7842), mouse antiglucagon antibody (Sigma, St. Louis, MO, Cat# G2654), rabbit antisomatostatin antibody (Abcam, Cat#ab103790), rabbit anti-p-Smad2/3 antibody (Santa Cruz, Cat# sc-11769R), rabbit anti-p-Smad1/5/8 antibody, (Santa Cruz, Cat# sc-12353R), rabbit anti-Ki67 antibody (Dako, Carpinteria, CA, Cat# M7249). The ratios of insulin-positive β-cells, glucagon-positive α-cells, and somatostatin-positive δ-cells to total islet cells were calculated from 40× images. All islets were imaged, and total β-cell number counted by counting nuclei surrounded by cytoplasmic insulin staining, total α-cell and δ-cell were counted in a similar method. For each mouse, about 10,000 β-cells were counted, and the β-cell proliferation ratio was calculated by dividing Ki67+ cell number by the total β-cell number.

Islet isolation and Western blot. To isolate islets, we first clamped the ampulla with surgical thread on the duodenum wall to block the bile pathway to the duodenum. Then, we injected 3 ml of Collagenase P enzyme (Sigma, C9263) at 0.5 mg/ml in a modified Hank's balanced salt solution (Invitrogen, Carlsbad, CA) into the pancreas via the common bile duct to distend the pancreas. The pancreas was then excised whole and placed in modified Hank's balanced salt solution for stationary digestion at 37 °C for 15 minutes. Ficoll 400 (Sigma, Cat # F4375) was used at different densities to purify islets from acinar tissue.

Islets protein was extracted using lysis buffer (1% Triton X-100, 0.1% SDS, 0.25% sodium deoxycholate, 150 mmol/l Tris (pH 7.5), 150 mmol/l NaCl, 1 mmol/l EDTA) with phosphatase inhibitor (Sigma, Cat # P0044) and protease inhibitor (Sigma, Cat# P0044). Total protein was quantitated using a BCA kit (Pierce, Cat# 23227). Twenty micrograms of protein per lane and prestained molecular weight markers (Bio-Rad, Hercules, CA, Cat#161–0318) were separated with 12% SDS/PAGE gels and transferred to polyvinylidene fluoride membranes. Membranes were blocked at room temperature for 1 hour with blocking solution containing 5% nonfat dried milk in 10 mmol/l Tris–Cl (pH 7.5), 100 mmol/l NaCl, and 0.1% Tween-20 (TBS-T). Membranes were then incubated overnight at 4 °C with primary antibodies (rabbit anti-p-Akt (Ser473) Cell Signaling, Beverly, MA, Cat#9271), Akt (Cell Signaling, Cat#9272), p-PI3K p85 (Cell Signaling, Cat#4228S) and GAPDH (Sigma, Cat#G9545), followed by secondary antibody incubation and developed with horseradish peroxidase-enhanced chemiluminescence.

Quantitative real-time PCR and real-time PCR array. Total RNA from the pancreas was extracted using TRIzol reagent (Invitrogen, Cat # 15596-018). The cDNA was synthesized using Superscript III First Strand cDNA synthesis kit (Invitrogen, Cat# 18080-051). For quantitative real-time PCR, SYBR green-based method was used for individual targeted genes. Primer sequences are described in **Supplementary Table S1**. The GUSB (β-glucuronidase) (Applied Biosystems, Grand Island, NY, Mm00446953_m1) was used as the endogenous control. The reaction was performed using the ABI 7300 real-time PCR system. The relative mRNA expression levels were calculated by the cycle threshold method ($\delta - \delta$Ct).

TGF-β/BMP signaling pathway PCR array was purchased from QIAGEN (TGFb BMP Signaling Pathway RT^2 Profiler PCR Array, Cat. No: PAMM-035Z, Venlo, The Netherlands). The cDNA synthesis, PCR assembly, and data analysis were strictly followed according to the manufacturer's protocol.

In vitro *reporter assay.* The mouse betatrophin promoter was cloned out with PCR method using a mouse liver sample. The primers used were 5′-AGC TGA CGC GTG AAA TTG AGG CTG TGT GGG-3′ and 5′-TCA CGA CCT GCA GGA GGC AGA GAG CAA GCA C-3′. After restriction digest with enzymes PstI and SbfI, the cDNA fragment was cohesively ligated to the pxxLxp3.3 plasmid (originated in our lab) containing the cytomegalovirus promoter and secretable gaussia luciferase. The final construct was designated as pxxLxp3.3-Betatrophin-Luc (Beta-Luc). The NIT-1 cells were plated in 24-well plates 1 day before transfection. Each well was transfected with 0.7 μg of the reporter vector Beta-Luc and 0.7 μg pAAV2.1-CB-LacZ plasmid for normalization using AG Transgen Transfection Reagent (Cat# AGT002). Six hours after transfection, the transfection media was replaced with conditional media containing activin (ACT), FST, myostatin (Myo), ACT+FST, Myo+FST or control bluescript plasmid (pBSKS, 1/3 of the indicated conditioned media + 0.5% FBS + 1 mmol/l sodium pyruvate). The media was harvested at different time points for Gaussia-Luc analysis. The activity of Gaussia-luc was determined using the BioLux Gaussia Luciferase Flex Assay Kit (BioLabs, Cat#E3308L) according to the manufacturer's instructions. LacZ activity was measured using a classic colorimetric ortho-nitrophenyl-β-galactoside (ONPG) assay method.[54] Calculation of luciferase activity was normalized to LacZ activity. All assays were performed at least in triplicate.

Statistical analysis. Values are expressed as mean ± SEM. Welch's *t*-test was applied when comparing two groups. When comparing three groups, one-way analysis of variance (ANOVA) plus Dunnett post-test was applied using Graph Pad Prism software. $P < 0.05$ was considered statistically significant.

SUPPLEMENTARY MATERIAL

Figure S1. Immunofluorescence staining of phosphor-SMAD1/5/8 in the pancreas.

Figure S2. The metabolism was slower in AAV8-Ins-FST treated db/db mice measured by indirect gas calorimetry system (CaloSys).

Table S1. The oligonucleotide primer sequences for real-time PCR.

ACKNOWLEDGMENTS

This work was supported by grants from the National Institutes of Health (DK-090380 and AR-056394). Our paraffin sections were performed in UNC CGIBD histology core, supported by P30 DK 034987 to Robert Sandler and Temitope Keku.

No potential conflicts of interest relevant to this article were reported.

REFERENCES

1. Narain, JP, Garg, R and Fric, A (2011). Non-communicable diseases in the South-East Asia region: burden, strategies and opportunities. *Natl Med J India* **24**: 280–287.
2. Lee, IM, Shiroma, EJ, Lobelo, F, Puska, P, Blair, SN and Katzmarzyk, PT; Lancet Physical Activity Series Working Group (2012). Effect of physical inactivity on major non-communicable diseases worldwide: an analysis of burden of disease and life expectancy. *Lancet* **380**: 219–229.
3. Aguilar, RB (2011). Evaluating treatment algorithms for the management of patients with type 2 diabetes mellitus: a perspective on the definition of treatment success. *Clin Ther* **33**: 408–424.
4. Israili, ZH (2011). Advances in the treatment of type 2 diabetes mellitus. *Am J Ther* **18**: 117–152.
5. Levy, J, Atkinson, AB, Bell, PM, McCance, DR and Hadden, DR (1998). Beta-cell deterioration determines the onset and rate of progression of secondary dietary failure in type 2 diabetes mellitus: the 10-year follow-up of the Belfast Diet Study. *Diabet Med* **15**: 290–296.
6. Bagust, A and Beale, S (2003). Deteriorating beta-cell function in type 2 diabetes: a long-term model. *QJM* **96**: 281–288.
7. Brown, DX and Evans, M (2012). Choosing between GLP-1 Receptor Agonists and DPP-4 Inhibitors: A Pharmacological Perspective. *J Nutr Metab* **2012**: 381713.
8. Ahrén, B (2011). GLP-1 for type 2 diabetes. *Exp Cell Res* **317**: 1239–1245.
9. Parkes, DG, Mace, KF and Trautmann, ME (2013). Discovery and development of exenatide: the first antidiabetic agent to leverage the multiple benefits of the incretin hormone, GLP-1. *Expert Opin Drug Discov* **8**: 219–244.
10. Kulkarni, RN, Mizrachi, EB, Ocana, AG and Stewart, AF (2012). Human β-cell proliferation and intracellular signaling: driving in the dark without a road map. *Diabetes* **61**: 2205–2213.
11. Bilezikjian, LM, Blount, AL, Leal, AM, Donaldson, CJ, Fischer, WH and Vale, WW (2004). Autocrine/paracrine regulation of pituitary function by activin, inhibin and follistatin. *Mol Cell Endocrinol* **225**: 29–36.
12. Nakamura, T, Takio, K, Eto, Y, Shibai, H, Titani, K and Sugino, H (1990). Activin-binding protein from rat ovary is follistatin. *Science* **247**: 836–838.
13. Patel, K (1998). Follistatin. *Int J Biochem Cell Biol* **30**: 1087–1093.
14. Kota, J, Handy, CR, Haidet, AM, Montgomery, CL, Eagle, A, Rodino-Klapac, LR *et al.* (2009). Follistatin gene delivery enhances muscle growth and strength in nonhuman primates. *Sci Transl Med* **1**: 6ra15.
15. Rodino-Klapac, LR, Haidet, AM, Kota, J, Handy, C, Kaspar, BK and Mendell, JR (2009). Inhibition of myostatin with emphasis on follistatin as a therapy for muscle disease. *Muscle Nerve* **39**: 283–296.
16. Gilson, H, Schakman, O, Kalista, S, Lause, P, Tsuchida, K and Thissen, JP (2009). Follistatin induces muscle hypertrophy through satellite cell proliferation and inhibition of both myostatin and activin. *Am J Physiol Endocrinol Metab* **297**: E157–E164.
17. Lee, SJ, Reed, LA, Davies, MV, Girgenrath, S, Goad, ME, Tomkinson, KN *et al.* (2005). Regulation of muscle growth by multiple ligands signaling through activin type II receptors. *Proc Natl Acad Sci USA* **102**: 18117–18122.
18. Wiater, E and Vale, W (2012). Roles of activin family in pancreatic development and homeostasis. *Mol Cell Endocrinol* **359**: 23–29.
19. Hashimoto, O and Funaba, M (2011). Activin in glucose metabolism. *Vitam Horm* **85**: 217–234.
20. Florio, P, Luisi, S, Marchetti, P, Lupi, R, Cobellis, L, Falaschi, C *et al.* (2000). Activin A stimulates insulin secretion in cultured human pancreatic islets. *J Endocrinol Invest* **23**: 231–234.
21. Yadav, H, Quijano, C, Kamaraju, AK, Gavrilova, O, Malek, R, Chen, W *et al.* (2011). Protection from obesity and diabetes by blockade of TGF-β/Smad3 signaling. *Cell Metab* **14**: 67–79.
22. Rehman, KK, Wang, Z, Bottino, R, Balamurugan, AN, Trucco, M, Li, J *et al.* (2005). Efficient gene delivery to human and rodent islets with double-stranded (ds) AAV-based vectors. *Gene Ther* **12**: 1313–1323.
23. Chen, H, Charlat, O, Tartaglia, LA, Woolf, EA, Weng, X, Ellis, SJ *et al.* (1996). Evidence that the diabetes gene encodes the leptin receptor: identification of a mutation in the leptin receptor gene in db/db mice. *Cell* **84**: 491–495.
24. Wang, Z, Zhu, T, Rehman, KK, Bertera, S, Zhang, J, Chen, C *et al.* (2006). Widespread and stable pancreatic gene transfer by adeno-associated virus vectors via different routes. *Diabetes* **55**: 875–884.
25. Brown, ML, Kimura, F, Bonomi, LM, Ungerleider, NA and Schneyer, AL (2011). Differential synthesis and action of TGFß superfamily ligands in mouse and rat islets. *Islets* **3**: 367–375.
26. Kumar, A (2012). Second line therapy: type 2 diabetic subjects failing on metformin GLP-1/DPP-IV inhibitors versus sulphonylurea/insulin: for GLP-1/DPP-IV inhibitors. *Diabetes Metab Res Rev* **28(Suppl 2)**: 21–25.
27. Yi, P, Park, JS and Melton, DA (2013). Betatrophin: a hormone that controls pancreatic β cell proliferation. *Cell* **153**: 747–758.
28. Chera, S, Baronnier, D, Ghila, L, Cigliola, V, Jensen, JN, Gu, G *et al.* (2014). Diabetes recovery by age-dependent conversion of pancreatic δ-cells into insulin producers. *Nature* **514**: 503–507.
29. Shimmi, O and Newfeld, SJ (2013). New insights into extracellular and post-translational regulation of TGF-β family signalling pathways. *J Biochem* **154**: 11–19.
30. Massaous, J and Hata, A (1997). TGF-beta signalling through the Smad pathway. *Trends Cell Biol* **7**: 187–192.
31. Wrighton, KH, Lin, X and Feng, XH (2009). Phospho-control of TGF-beta superfamily signaling. *Cell Res* **19**: 8–20.
32. Cantley, LC (2002). The phosphoinositide 3-kinase pathway. *Science* **296**: 1655–1657.
33. Forbes, D, Jackman, M, Bishop, A, Thomas, M, Kambadur, R and Sharma, M (2006). Myostatin auto-regulates its expression by feedback loop through Smad7 dependent mechanism. *J Cell Physiol* **206**: 264–272.
34. Onichtchouk, D, Chen, YG, Dosch, R, Gawantka, V, Delius, H, Massagué, J *et al.* (1999). Silencing of TGF-beta signalling by the pseudoreceptor BAMBI. *Nature* **401**: 480–485.
35. Zhu, J, Lin, SJ, Zou, C, Makanji, Y, Jardetzky, TS and Woodruff, TK (2012). Inhibin α-subunit N terminus interacts with activin type IB receptor to disrupt activin signaling. *J Biol Chem* **287**: 8060–8070.
36. Makanji, Y, Walton, KL, Wilce, MC, Chan, KL, Robertson, DM and Harrison, CA (2008). Suppression of inhibin A biological activity by alterations in the binding site for betaglycan. *J Biol Chem* **283**: 16743–16751.
37. Loveland, KL, Bakker, M, Meehan, T, Christy, E, von Schönfeldt, V, Drummond, A *et al.* (2003). Expression of Bambi is widespread in juvenile and adult rat tissues and is regulated in male germ cells. *Endocrinology* **144**: 4180–4186.
38. Hua, H and Sarvetnick, N (2007). ID2 promotes the expansion and survival of growth-arrested pancreatic beta cells. *Endocrine* **32**: 329–337.
39. Sidis, Y, Mukherjee, A, Keutmann, H, Delbaere, A, Sadatsuki, M and Schneyer, A (2006). Biological activity of follistatin isoforms and follistatin-like-3 is dependent on differential cell surface binding and specificity for activin, myostatin, and bone morphogenetic proteins. *Endocrinology* **147**: 3586–3597.
40. Mukherjee, A, Sidis, Y, Mahan, A, Raher, MJ, Xia, Y, Rosen, ED *et al.* (2007). FSTL3 deletion reveals roles for TGF-beta family ligands in glucose and fat homeostasis in adults. *Proc Natl Acad Sci USA* **104**: 1348–1353.
41. Brown, ML, Bonomi, L, Ungerleider, N, Zina, J, Kimura, F, Mukherjee, A *et al.* (2011). Follistatin and follistatin like-3 differentially regulate adiposity and glucose homeostasis. *Obesity (Silver Spring)* **19**: 1940–1949.
42. Lin, HM, Lee, JH, Yadav, H, Kamaraju, AK, Liu, E, Zhigang, D *et al.* (2009). Transforming growth factor-beta/Smad3 signaling regulates insulin gene transcription and pancreatic islet beta-cell function. *J Biol Chem* **284**: 12246–12257.
43. El-Gohary, Y, Tulachan, S, Wiersch, J, Guo, P, Welsh, C, Prasadan, K *et al.* (2014). A smad signaling network regulates islet cell proliferation. *Diabetes* **63**: 224–236.
44. Smart, NG, Apelqvist, AA, Gu, X, Harmon, EB, Topper, JN, MacDonald, RJ *et al.* (2006). Conditional expression of Smad7 in pancreatic beta cells disrupts TGF-beta signaling and induces reversible diabetes mellitus. *PLoS Biol* **4**: e39.
45. Casellas, R and Brivanlou, AH (1998). Xenopus Smad7 inhibits both the activin and BMP pathways and acts as a neural inducer. *Dev Biol* **198**: 1–12.
46. Xiao, X, Wiersch, J, El-Gohary, Y, Guo, P, Prasadan, K, Paredes, J *et al.* (2013). TGFβ receptor signaling is essential for inflammation-induced but not β-cell workload-induced β-cell proliferation. *Diabetes* **62**: 1217–1226.
47. Elghazi, L, Rachdi, L, Weiss, AJ, Cras-Méneur, C and Bernal-Mizrachi, E (2007). Regulation of beta-cell mass and function by the Akt/protein kinase B signalling pathway. *Diabetes Obes Metab* **9(Suppl 2)**: 147–157.
48. Elghazi, L and Bernal-Mizrachi, E (2009). Akt and PTEN: beta-cell mass and pancreas plasticity. *Trends Endocrinol Metab* **20**: 243–251.
49. Oliveira, JM, Rebuffat, SA, Gasa, R and Gomis, R (2014). Targeting type 2 diabetes: lessons from a knockout model of insulin receptor substrate 2. *Can J Physiol Pharmacol* **92**: 613–620.
50. Gunton, JE, Kulkarni, RN, Yim, S, Okada, T, Hawthorne, WJ, Tseng, YH *et al.* (2005). Loss of ARNT/HIF1beta mediates altered gene expression and pancreatic-islet dysfunction in human type 2 diabetes. *Cell* **122**: 337–349.
51. Kadowaki, T, Tamemoto, H, Tobe, K, Terauchi, Y, Ueki, K, Kaburagi, Y *et al.* (1996). Insulin resistance and growth retardation in mice lacking insulin receptor substrate-1 and identification of insulin receptor substrate-2. *Diabet Med* **13**(*9* Suppl *6*): S103–S108.
52. Ayuso, E, Mingozzi, F, Montane, J, Leon, X, Anguela, XM, Haurigot, V *et al.* (2010). High AAV vector purity results in serotype- and tissue-independent enhancement of transduction efficiency. *Gene Ther* **17**: 503–510.
53. Qiao, C, Li, J, Jiang, J, Zhu, X, Wang, B, Li, J *et al.* (2008). Myostatin propeptide gene delivery by adeno-associated virus serotype 8 vectors enhances muscle growth and ameliorates dystrophic phenotypes in mdx mice. *Hum Gene Ther* **19**: 241–254.
54. Qiao, C, Wang, B, Zhu, X, Li, J and Xiao, X (2002). A novel gene expression control system and its use in stable, high-titer 293 cell-based adeno-associated virus packaging cell lines. *J Virol* **76**: 13015–13027.